A R C H I V E O F M E C H A N I C A L E N G I N E E R I N G

VOL. LXIV 2017 Number 1

DOI: 10.1515/meceng-2017-0005

Key words: labyrinth seal, metamodel optimization, neural network, genetic algorithms, evolutionary algorithms, CFD optimization

SEBASTIAN RULIK[1], *WŁODZIMIERZ WRÓBLEWSKI*[1], *DANIEL FRĄCZEK*[1]

METAMODEL-BASED OPTIMIZATION OF THE LABYRINTH SEAL

The presented paper concerns CFD optimization of the straight-through labyrinth seal with a smooth land. The aim of the process was to reduce the leakage flow through a labyrinth seal with two fins. Due to the complexity of the problem and for the sake of the computation time, a decision was made to modify the standard evolutionary optimization algorithm by adding an approach based on a metamodel. Five basic geometrical parameters of the labyrinth seal were taken into account: the angles of the seal's two fins, and the fin width, height and pitch. Other parameters were constrained, including the clearance over the fins. The CFD calculations were carried out using the ANSYS-CFX commercial code. The in-house optimization algorithm was prepared in the Matlab environment. The presented metamodel was built using a Multi-Layer Perceptron Neural Network which was trained using the Levenberg-Marquardt algorithm. The Neural Network training and validation were carried out based on the data from the CFD analysis performed for different geometrical configurations of the labyrinth seal. The initial response surface was built based on the design of the experiment (DOE). The novelty of the proposed methodology is the steady improvement in the response surface goodness of fit. The accuracy of the response surface is increased by CFD calculations of the labyrinth seal additional geometrical configurations. These configurations are created based on the evolutionary algorithm operators such as selection, crossover and mutation. The created metamodel makes it possible to run a fast optimization process using a previously prepared response surface. The metamodel solution is validated against CFD calculations. It then complements the next generation of the evolutionary algorithm.

Nomenclature

a – selected design variable, [variable unit]
a_l, a_u – lower and upper range of limits for the selected design variable, [variable unit]
A – cross-section area of passing fluid, [m^2]
b – parameter specifying the non-uniform rate ($b = 2$), [–]

[1] *Silesian University of Technology, Institute of Power Engineering and Technology, Konarskiego 18 Str., 44-100 Gliwice, Poland. Emails: sebastian.rulik@polsl.pl, wlodzimierz.wroblewski@polsl.pl, daniel.fraczek@polsl.pl*

c_d – discharge coefficient, [–]
$\dot{m}$ – mass flow-rate, [kg/s]
p_{tot_in} – inlet total pressure, [Pa]
R – specific gas constant,[J/(kg K)]
r – number of initial vectors, [–]
s – random number between 0 and 1, [–]
t – generation number, [–]
T – maximum number of generations, [–]
T_{tot_in} – inlet total temperature, [K]

Greek symbols

α – scaling factor, [–]
π – ratio of inlet total pressure to outlet static pressure, [–]
κ – specific heat ratio, [–]

1. Introduction

Labyrinth seals are one of the main components of the gas turbine. They are fairly efficient and ensure the machine long life at a relatively simple structure. Due to design, strength and thermal limitations, different types of labyrinth seals are applied in the gas turbine, e.g. straight-through seals, stepped convergent seals and stepped divergent seals. Each of these may be configured with a smooth or a honeycomb land. The basic function of the gas turbine sealing is leakage reduction or control. The reduction in leakage is the most essential in the area of the turbine main flow, especially above the rotor blades. The tip seal leakage flow does not participate in power generation and is an additional source of losses arising due to the process of mixing with the main flow. The control function of the sealing is used to obtain a correct spread of cooling air. Therefore, designing a labyrinth seal that will best fulfil its functions is an issue of great importance. Due to complex flow phenomena occurring in the seal cavities, appropriate selection of geometrical features is not an easy task. In order to meet a number of design requirements, those geometrical characteristics can only be found using more sophisticated design tools based on 3D flow modelling and optimization algorithms.

Nowadays, nondeterministic methods such as genetic algorithms are used in the optimization process. Genetic algorithms are substantially different from traditional methods. One of the differences is that an entire population of points, not just one single point, is taken into consideration in the space of possible solutions [1]. The algorithms take account of the element of randomness and mimic real biological processes. This gives them natural resistance to getting stuck in a local optimum. Their another advantage, resulting from their structure, is the opportunity to perform parallel computations.

A comprehensive study using a genetic algorithm and devoted to the search for the optimum geometry of the stepped labyrinth seal can be found in [2]. In [3], a more complex geometry of a seal with a honeycomb land is optimized by

means of a genetic algorithm. A simplified geometry of the honeycomb is adopted in this case, which makes it possible to substantially reduce the geometrical mesh size and, consequently, to carry out a full optimization process. Another example of optimization drawing on genetic algorithms are works [4, 5], which concern the thermal and flow optimization of the turbine blades cooling system.

The application of genetic algorithms involves the need of calculating a very large number of cases. Considering that some CFD computations are extremely time-consuming, such algorithms may prove ineffective or even impossible to use. For this reason, metamodel-based optimization techniques are now being developed intensively. This approach significantly limits the number of the calculations of the objective functions. An example of optimization using a response surface constructed based on the Design of Experiment (DOE) is presented in [6], where a commercial FEM code is used to optimize the shape of the rotor blades of a supercritical steam turbine. However, using a metamodel increases the risk of finding a local optimum only. This happens if the metamodel is built using too few tests in the DOE or if the analysed problem happens to be strongly nonlinear, with a large number of local optimums. An interesting combination of a traditional genetic algorithm with the metamodel-based optimization is presented in [7], where the Real-Coded Population Dispersion (RCPD) genetic algorithm is applied. The obtained results were used for subsequent populations to build a response surface based on a Neural Network. This approach enables a gradual improvement in the metamodel goodness of fit, bringing its solutions closer to the real results obtained by means of a numerical analysis. It is possible to fill the solution space uniformly owing to an analysis of results conducted with the use of the normal distribution. Based on the distribution, it is also found in which case the objective function is determined by means of the metamodel, and in which case it is calculated using a rather time-consuming numerical analysis.

Quite a similar approach is put forward herein, but with a few essential modifications. Here, the developed algorithm is based on a traditional genetic algorithm, where some individuals are generated additionally using a metamodel based on an artificial Neural Network. The applied methodology thus makes it possible to combine the advantages and avoid the downsides of the two methods. The presented algorithm is used to calculate a simple geometry of a straight-through labyrinth seal with a smooth land, which makes it possible to verify the algorithm and check its suitability for solving the kind of problems currently discussed. It is planned that the algorithm will be used in further calculations of the seal complex three-dimensional geometries, taking account of the honeycomb structure and its optimization.

2. Optimization algorithm

The optimization process was carried out using an in-house code developed in the Matlab environment. The algorithm is a considerable extension of the method used in [3]. It co-operates with the Ansys-CFX 15 commercial code used for CFD

analyses. The generation process of the geometry and the numerical mesh as well as of the definition of boundary conditions is completely automatic and it is run in the Ansys-Workbench environment. The algorithm makes it possible to perform optimization computations on many computers in parallel, which significantly improves its efficiency.

The applied optimization algorithm is composed of two basic modules. One of them is the main genetic algorithm based on encoding with real-valued numbers. The other is an additional module – a Neural Network creating what is referred to as the response surface, which is used in an additional optimization process. The obtained results are then verified based on CFD calculations and they supply the population of the main genetic algorithm. The points that make up the response surface are built based on the genetic algorithm subsequent generations. In this way, the response surface goodness of fit is gradually improved, bringing the solutions obtained by means of the metamodel closer to real solutions derived from a CFD analysis. A flowchart of the optimization algorithm operation is shown in Fig. 1.

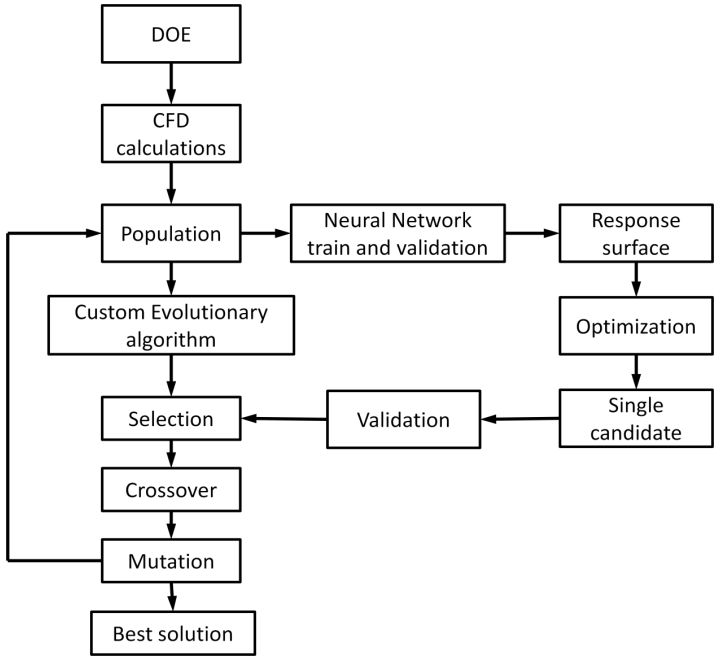

Fig. 1. Optimization algorithm flowchart

One of the differences compared to a traditional genetic algorithm is the replacement of the initial random distribution of design variables with a distribution obtained using the DOE. This approach makes it possible to fill the solution space uniformly. The presented algorithm makes use of the central composite design of the experiment [8, 9]. The design is created from two-level fractional designs

supplemented with star points and centre points. In the star points, individual variables are changed one by one on two levels $\pm a$, keeping the other variables at level 0. The star points lie on coordinate axes and they are arranged symmetrically – two on each axis at the distance of $\pm a$ from the design centre. The a quantities for individual design variables are often called the star radii.

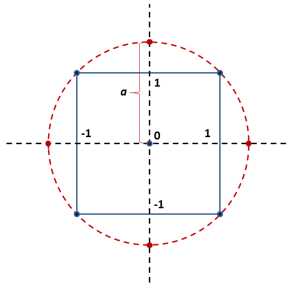

Fig. 2. Composite design for two standardized variables

An example composite design for two standardized variables is presented in Fig. 2. An application of the fractional factorial design for 5 design variables gives the total of 27 combinations of their values. The results obtained based on the experiment design constitute the first population of the genetic algorithm and are used to build a metamodel.

The metamodel is constructed using a Multi-Layer Perceptron Neural Network with a single hidden layer (cf. Fig. 3). In this case, the input vector are five design variables constituting individual geometrical parameters of the seal, whereas the output vector is a single value of the discharge coefficient determined based on the labyrinth seal leakage mass flow (cf. Fig. 3).

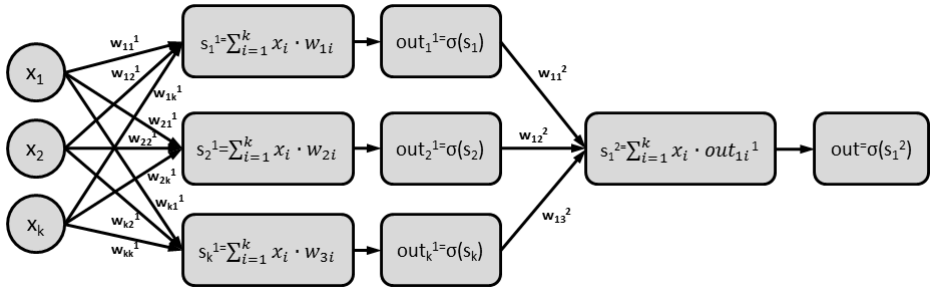

Fig. 3. Structure of the Neural Network used to build the metamodel

A sigmoidal activation function σ is used for the hidden layer of neurons, whereas for the output layer – a linear activation function is adopted. The selection of the Neural Network weights is based on the Levenberg-Marquardt backpropagation algorithm [10]. A metamodel built in this way makes it possible to run the

optimization process on the obtained response surface. For this purpose, a default genetic algorithm implemented in the Matlab environment is used. It is assumed that computations may be run for several different numbers of neurons used in the Neural Network hidden layer, which gives several possible solutions validated further on based on CFD calculations. The results obtained in this manner are the first approximation of the global minimum.

The proposed algorithm novelty is the gradual improvement in the response surface goodness of fit, which is achieved using individuals from subsequent generations of the main genetic algorithm. Subsequent populations of individuals are generated using the genetic algorithm operators such as selection, crossover and mutation. The generated individuals are additionally supplemented with optimal solutions obtained from the optimization process run with the use of the metamodel. The whole constitutes a new population for which CFD calculations are performed and, thereby, the fitness function is determined. At the same time, the calculations enable validation of results obtained by means of the metamodel-based optimization. The obtained results make it possible to construct an improved metamodel, thus improving the response surface goodness of fit based on a bigger number of data.

An application of the genetic algorithm operators enables data concentration in the global optimum area and ensures the response surface better goodness of fit, especially in this region.

It is assumed that the applied operators of the genetic algorithm are based on encoding by means of real-valued numbers. The extended intermediate recombination algorithm is adopted for the crossover process. In this case, the values of the offspring individual chromosomes are either included between the values of both parents or are close to them, which means that the offspring is generated according to the following principle [11]:

$$\begin{aligned} \text{offspring}_1 &= \text{parent}_1 + \alpha(\text{parent}_2 - \text{parent}_1) \\ \text{offspring}_2 &= \text{parent}_2 + \alpha(\text{parent}_2 - \text{parent}_1) \end{aligned} \tag{1}$$

where α is a scaling factor chosen uniformly at random over an interval $[-d, 1+d]$. For the extended intermediate recombination it is assumed that $d = 0.25$. The use of extended recombination prevents shrinking of the interval of a given parameter variability in subsequent generations.

For the mutation process, a non-uniform mutation factor dependent on the generation number is assumed. At the beginning, the mutation factor is high but its value decreases as subsequent iterations proceed. This kind of approach helps the evolutionary algorithm to fit the global optimum better. The mutation factor is defined by the following formula [12]:

$$\Delta(t, y) = y(1 - s^{((1-t/T)/b)}) \tag{2}$$

where $y = a - a_l$ for random number equal to 1, $y = a_u - a$ for random number equal to 0.

The new design variable a' is calculated from the following relation:

$$a' = \begin{cases} a + \Delta(t, y) \\ a - \Delta(t, y) \end{cases} \tag{3}$$

An additional function is used in the proposed algorithm to scale the obtained results, which improves the selection process. It is assumed that results are scaled using the flow maximum value in a given generation.

3. Numerical model of the labyrinth seal

The subject of the numerical analysis is the model of the gas turbine rotor tip seal. The labyrinth seal has two fins. Only the seal smooth land option is analysed and the honeycomb land structure is omitted. The labyrinth seal initial geometry is shown in Fig. 4.

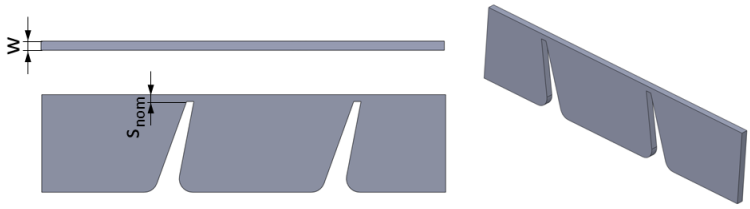

Fig. 4. Labyrinth seal geometry

It is assumed that the optimization process is run for a single dimension of the clearance – s_{nom} = 0.76 mm. The computational domain width is assumed as w = 0.25 mm. The other dimensions of the seal and the flow parameters correspond to the data of the measuring stand in the Institute of Power Engineering and Turbomachinery of the Silesian University of Technology. It is a stationary test rig that operates under vacuum pressure and is fed with atmospheric air. For the seal under analysis, only the axial inflow of air is taken into consideration. It is further assumed that the computational domain is stationary. The numerical analysis is conducted by means of the Ansys-CFX 15 commercial program. The basic boundary conditions assumed for the calculations are listed in Table 1.

Table 1.

Boundary conditions assumed for the analysis

Boundary conditions		Value
Inlet	Total pressure	100 kPa
	Total temperature	20°C
Outlet	Average static pressure	86.2 kPa

The high-resolution advection scheme is set up for continuity, energy, momentum and turbulence equations. The gas properties are set up as air ideal gas

with the total energy heat transfer option. The two-equation Shear Stress Transport turbulence model is applied.

In order to determine the seal performance, a dimensionless discharge coefficient – c_D – is introduced. The coefficient is defined according to (4).

$$c_D = \frac{\dot{m}}{\dot{m}_{id}} \tag{4}$$

The coefficient describes the ratio of the leakage mass flow to the ideal mass flow. The ideal mass flow is a theoretical quantity for isentropic expansion through a single nozzle [13]:

$$\dot{m}_{id} = \frac{\dot{Q}_{id} p_{tot\_in} A}{\sqrt{T_{tot\_in}}}$$
$$\dot{Q}_{id} = \sqrt{\frac{2\kappa}{R(\kappa-1)}\left[1-\left(\frac{1}{\pi}\right)^{\frac{\kappa-1}{\kappa}}\right]}\left(\frac{1}{\pi}\right)^{\frac{1}{\kappa}} \tag{5}$$

The numerical mesh adopted for the optimization process is shown in Fig. 5. It was generated using the Ansys-Meshing program. The generation process is automatic and its parameters for all analysed configurations of the seal are identical. The mesh is of the hexa-dominant type and it is composed of about 138 thousand nodes. The mesh is extended to the distance of 0.25 mm in the normal direction and contains a single element only. This makes the analysis a two-dimensional one. The circumferential component of velocity was omitted and only an axial component was taken into account. However, this approach is often used in literature concerning both numerical and experimental studies [2, 13]. The density of the presented mesh is much higher in the fin tip area. The maximum value of the dimensionless quantity $y+$ does not exceed 1.

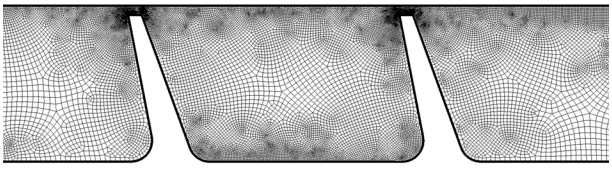

Fig. 5. Numerical mesh adopted for the calculations

Before the optimization process was started, an analysis of the solution independence of the numerical mesh was conducted. The obtained results showing the values of coefficient c_D are listed in Table 2. In total, 4 numerical meshes were investigated. The first three differ in the degree of concentration of elements in the fin area, whereas the last numerical mesh makes it possible to determine the impact of discretization in the direction normal to the one presented in Fig. 5. Due to the

comparatively small relative error, a decision was made to run the process of the labyrinth seal shape optimization using the initial mesh.

Table 2.

Impact of the numerical mesh

Type of mesh	Number of elements	c_D	Relative error, %
mesh 0 – adopted for optimization	130 000	0.590	0.3
mesh 1	188 000	0.595	0.5
mesh 2	293 000	0.596	0.7
mesh 2 – 5 layers in the normal direction	883 000	0.592	0

4. Optimization process

The basic parameters assumed in the optimization process using the presented optimization algorithm are listed in Table 3. The data concern the main genetic algorithm.

Table 3.

Basic parameters of the evolutionary algorithm

Evolutionary algorithm parameter	Value
Number of generations for the main genetic algorithm	40
Number of individuals in a population	24
Crossover probability for the main genetic algorithm	0.7
Mutation probability for the main genetic algorithm	0.02

A bigger number of individuals in a population (60) was assumed for the additional genetic algorithm operating in the response surface, and the maximum number of generations was increased. The other parameters were the same as those in the main genetic algorithm. The results obtained in this way were then verified based on CFD calculations. After that, they were added to the subsequent population of the main genetic algorithm. In each generation, the worst two geometrical configurations with the highest value of coefficient c_D were rejected.

Five geometrical parameters were taken into account in the optimization process: angles of the two fins, the fin height, width and pitch. They are all presented in Fig. 6. The calculations were performed for a constant clearance of 0.76 mm and for a constant taper angle of the fins.

The range of optimization-related changes in individual parameters together with the initial values are listed in Table 4.

Fig. 7 presents a comparison concerning the convergence process between a traditional genetic algorithm and its modified version using additional data obtained from optimization performed by means of the metamodel. The comparison concerns the entire population fitness function expressed as the total of coefficient c_D

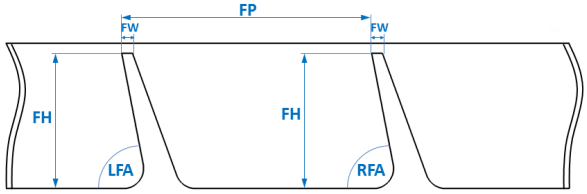

Fig. 6. Seal geometrical parameters under optimization

Table 4.

Range of optimized parameters variability

Parameter	Parameter limits
FW, mm	0.25 – 1.5
FH, mm	5 – 12
FP, mm	18 – 26
LFA, °	50 – 90
RFA, °	50 – 90

of all individuals being members of a given generation population. It can clearly be seen here that the proposed optimization algorithm is characterized by much better convergence compared to the traditional genetic algorithm. The metamodel-based genetic algorithm needed only 12 generations to achieve convergence, whereas in the case of the traditional genetic algorithm even 40 generations were not enough to do so. This characteristic is further proved by the obtained minimum value of discharge coefficient c_D, which is higher by about 2% for the traditional genetic algorithm. The fast convergence process of proposed optimization algorithm was possible owing to the use and validation of subsequent geometrical configura-

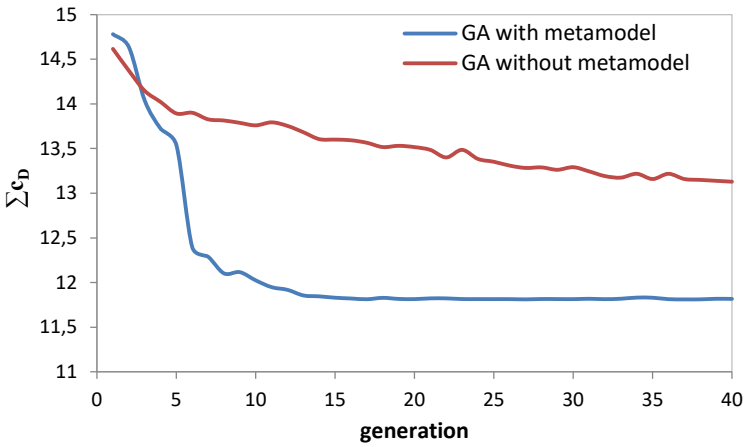

Fig. 7. Genetic algorithm convergence process

tions obtained based on the data from optimization performed by means of the metamodel.

Fig. 8 presents the response surface goodness of fit obtained based on data from 5 generations of the genetic algorithm, including the initial points obtained by means of the DOE. The presented data relate to the applied Neural Network both training and validation. It can be seen here that the applied Neural Network gives results that are very similar to those anticipated, which is proved by the trend line slope of almost 45°. Therefore, the optimum solution found by means of the response surface is very close to the one obtained after a verification process run using a CFD analysis. The solutions quickly dominate the genetic algorithm population, thus accelerating the algorithm convergence process.

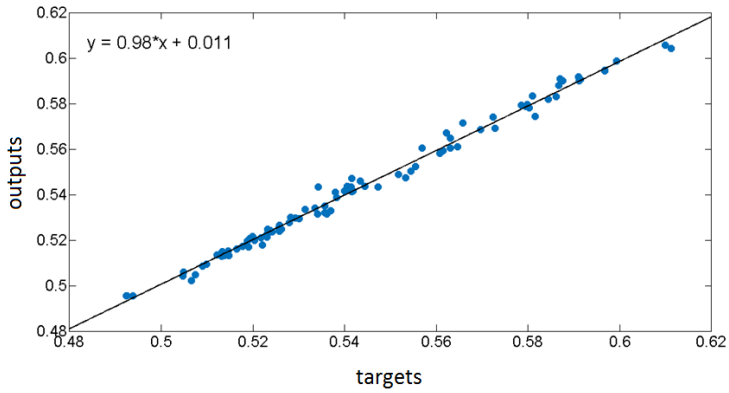

Fig. 8. Response surface goodness of fit

Table 5 presents a comparison between the initial and the optimized geometry. Discharge coefficient c_D is reduced here by more than 17% compared to the initial geometry. Except for the fin width, all optimized parameters reach limit values of the assumed intervals of variability. The left fin angle approaches the minimum value of 50°, whereas for the right one – the angle takes the maximum value of 900. The fin pitch and height have become bigger.

Table 5.

Initial and optimum parameters of the labyrinth seal geometry

Parameter	Initial geometry	Optimum geometry
FW, mm	0.8	0.264
FH, mm	10	12
FP, mm	18.55	26
LFA, °	79	50
RFA,°	79	90
c_D	**0.594**	**0.490**

Fig. 9 and Fig. 10, respectively, present a comparison of the flow field structure for the initial and optimum geometries. The inclination of the first fin causes that the vortex near the fin root is much bigger than for the initial geometry. The inclination of the left fin changes the direction of the leakage inflow into the clearance and causes a bigger contraction of the stream. The flow field structure in between the seal fins is also different. In the case of the optimum geometry, only one large vortex with a disturbed flow structure is formed in between the fins near the left fin tip. In the case of the initial geometry, two smaller vortices with a different degree of intensity are formed in between the fins. Furthermore, there is a significant decrease in the flow velocity over both the first and the second fin in the case of the optimum geometry.

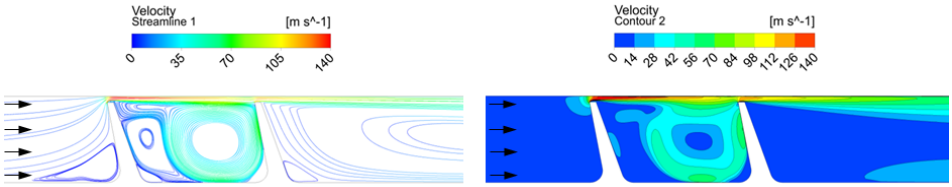

Fig. 9. Distribution of streamlines and the velocity field for the initial geometry

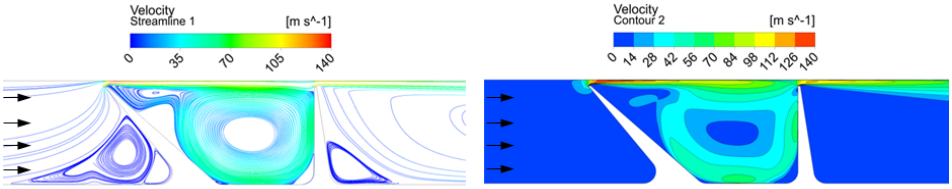

Fig. 10. Distribution of streamlines and the velocity field for the optimum geometry

Fig. 11 presents the pressure distribution along a single streamline for both the initial and the optimum geometry For the initial geometry, a higher pressure drop occurs on the first fin compared to the optimum geometry. The difference is about 2 kPa. This means that in the case of the optimum geometry the carry-over effect is smaller. Therefore, the pressure value in the space in between the fins is higher.

5. Sensitivity analysis

The sensitivity analysis was performed in two basic stages. Both concerned the global sensitivity analysis. The first stage included the use of a scatterplot-based graphical method, whereas the second stage of the sensitivity analysis was conducted using the Morris method [14].

The scatterplot-based graphical method involves visualization of all simulation points $\mathbf{X}^n, \mathbf{Y}^n$) in the form of a cloud presented in charts $\mathbf{X}_i - \mathbf{Y}_i$, $i = 1, d$,

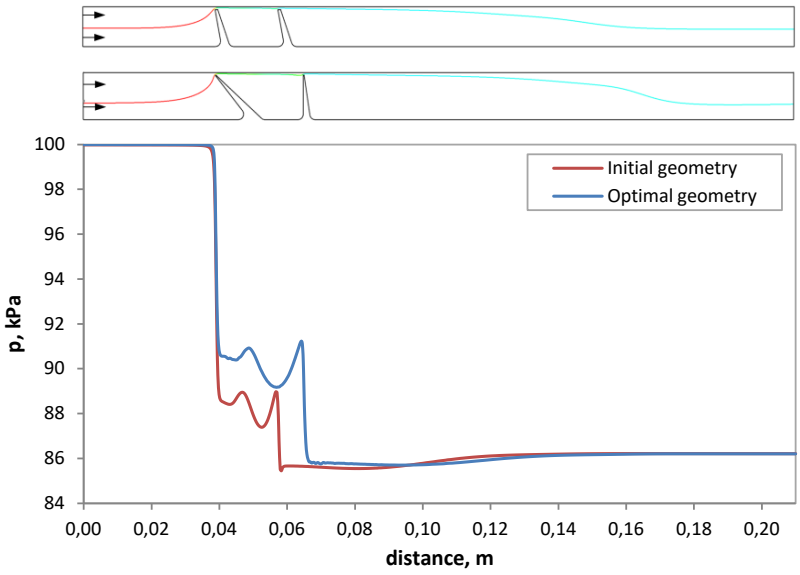

Fig. 11. Pressure distribution along the streamline

where d denotes the subsequent variable parameter of the simulation [15]. The charts obtained in this manner and illustrating the impact of individual geometrical parameters of the seal on the value of discharge coefficient c_D are shown in Fig. 12. Due to the fact that the charts were made using the data from the entire optimization process, the cloud of points is strongly concentrated in the area of the optimum solution. The parameters with the greatest impact on the discharge coefficient are the fin width (FW) and the fin pitch (FP). It can be seen here that the cloud of points is shifted distinctly downwards if the fin width gets smaller and if the fin pitch gets bigger. In the case of the sensitivity analysis of the impact of the fin height (FH), and of the right fin angle (RFA) in particular, it can be observed that the cloud of points is strongly dispersed, which means that the impact of these parameters on the objective function value is slight compared to the others. As for the left fin angle (LFA), the discharge coefficient value gets smaller as the angle decreases. Nevertheless, the impact of this parameter is smaller than that of parameters FW and FP.

The second stage of the sensitivity analysis was carried out using the Morris method [14]. It is a screening method based on discretization of analysed parameters into levels. The method enables a quick search of the space of possible solutions and determination of relationships between parameters, minimizing the number of necessary calculations at the same time. In it, each subsequent parameter is changed assuming that the other parameters are constant (“one-at-a-time” (OAT) design). The Morris method makes it possible to classify input variables into three groups. The first one comprises parameters with a slight impact only. The second group

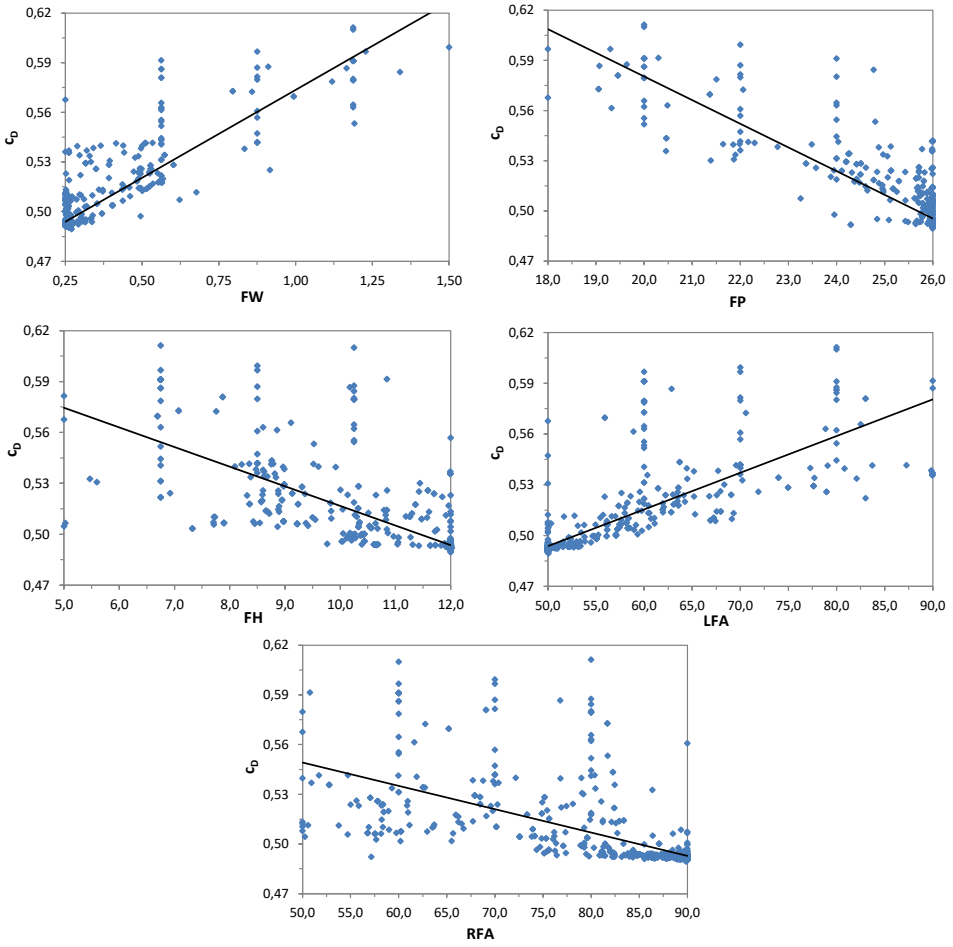

Fig. 12. Graphical illustration of the sensitivity of the objective function – discharge coefficient c_D – to a change in the seal individual geometrical parameters

includes parameters with a great linear impact that do not interact with the other parameters. The last group includes parameters with a strong nonlinear impact or those which involve strong interaction with the other parameters.

Taking r as the number of initial vectors $\mathbf{X}$, composed of the analysed parameters, and assuming that the parameter space is a d-dimensional mesh with n levels, the Elementary Effect may be defined as follows [15, 16]:

$$E_j^{(i)} = \frac{f(\mathbf{X}^{(i)} + \Delta e_j) - f(\mathbf{X}^{(i)})}{\Delta} \tag{6}$$

where: Δ is a predetermined multiple $\dfrac{1}{(n-1)}$ and e_j is a vector of the canonical base.

Additionally, two basic indices may be defined according to formulas (7) and (8) below. The first is the mean of the elementary effect absolute value for a given parameter, whereas the second is the standard deviation.

$$\mu_j^* = \frac{1}{r}\sum_{i=1}^{r}\left|E_j^{(i)}\right| \tag{7}$$

$$\sigma_j = \sqrt{\frac{1}{r}\sum_{i=1}^{r}\left(E_j^{(i)} - \frac{1}{r}\sum_{i=1}^{r}E_j^{(i)}\right)^2} \tag{8}$$

μ_j^* – the mean of the elementary effect is a measure of the effect of the j-th input on the output σ_j – the standard deviation is a measure of nonlinear and/or interaction effects of the j-th input [15].

No additional CFD calculations were performed in the presented analysis to determine the value of discharge coefficient c_D for individual vectors of initial parameters needed to conduct a sensitivity analysis. However, the previously developed metamodel using the optimization process data was applied. This enabled a parallel comparison between the sensitivity analysis conducted by means of a graphical method based on the real data from the CFD analysis and the sensitivity analysis performed by means of the Morris method based on the metamodel data. The Matlab toolbox for the global sensitivity analysis was used in the process [17].

Fig. 13 presents the values of elementary effects for individual parameters depending on their standard deviation. The obtained results coincide with the findings of the graphical analysis but they enable a better quantitative analysis of their impact.

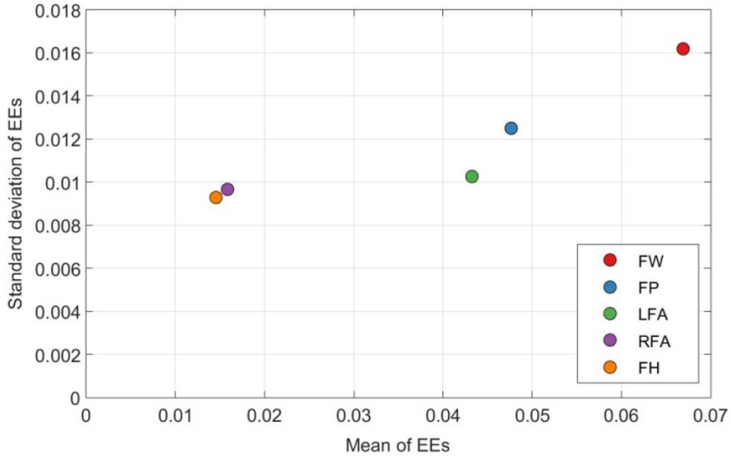

Fig. 13. Elementary effects depending on their standard deviation [17]

The results show that the parameter with the strongest impact on discharge coefficient c_D is the fin width (FW). This parameter also has a higher value of the standard deviation, which indicates that it may have a significant impact on the optimum values of the other parameters. The standard deviation values of the other parameters are similar to each other. Despite this, however, the impact of both the fin pitch (FP) and the left fin angle (LFA) is substantially bigger compared to the impact of the right fin angle (RFA) and the fin height (FH), which is proved by the mean of the elementary effect value, which is about three times higher.

6. Summary and conclusions

The basic aim of the work was to optimize the shape of the labyrinth tip seal using the Ansys-CFX commercial code and an in-house optimization algorithm. A novel approach was presented that combines the advantages of a traditional evolutionary algorithm with optimization run on a previously constructed metamodel, which shortens the computation time considerably. Five geometrical parameters of the seal were optimized. For each of them specific intervals of variation were assumed. The optimization process resulted in a reduction in discharge coefficient c_D. The coefficient value was by 17.5% smaller compared to the initial geometry. Moreover, the scatterplot graphical method and the Morris method were used to conduct a sensitivity analysis. Based on the two methods, one may conclude that the fin width and the fin pitch are the parameters with the greatest impact. The ones with the least impact are the fin height and the right fin angle. The developed optimization algorithm together with the conclusions drawn from the optimization process and the sensitivity analysis provide a basis for further investigations aiming to optimize the labyrinth seal shape, taking account of the honeycomb structure. In this case, however, it is necessary to perform a three-dimensional CFD analysis, which lengthens the computation time and requires an effective optimization algorithm. This will be the subject of further studies, both numerical and experimental.

Acknowledgements

This work was supported by the National Centre for Research and Development and Avio Polska within the Innolot Programm, project Coopernik.

Manuscript received by Editorial Board, October 07, 2016;
final version, December 28, 2016.

References

[1] G. Renner and A. Ekárt. Genetic algorithms in computer aided design. *Computer-Aided Design*, 35(8):709–726, 2003. doi: 10.1016/S0010-4485(03)00003-4.

[2] V. Schramm. *Labyrinth Seals of Maximum Sealing: A Approach to Computer-Based Form Optimization*, volume 46. Logos Verlag Berlin GmbH, 2011. (in German).

[3] W. Wróblewski, S. Dykas, K. Bochon, and S. Rulik. Optimization of tip seal with honeycomb land in LP counter rotating gas turbine engine. *Task Quarterly*, 14(3):189–207, 2010.

[4] G. Nowak and W. Wróblewski. Cooling system optimisation of turbine guide vane. *Applied Thermal Engineering*, 29(2-2):567–572, 2009. doi: 10.1016/j.applthermaleng.2008.03.015.

[5] G. Nowak, W. Wróblewski, and I. Nowak. Convective cooling optimization of a blade for a supercritical steam turbine. *International Journal of Heat and Mass Transfer*, 55(17-18):4511–4520, 2012. doi: 10.1016/j.ijheatmasstransfer.2012.03.072.

[6] G. Nowak and A. Rusin. Shape and operation optimisation of a supercritical steam turbine rotor. *Energy Conversion and Management*, 74:417–425, 2013. doi: 10.1016/j.enconman.2013.06.037.

[7] A. Jahangirian and A. Shahrokhi. Aerodynamic shape optimization using efficient evolutionary algorithms and unstructured CFD solver. *Computers & Fluids*, 46(1):270–276, 2011. doi: 10.1016/j.compfluid.2011.02.010.

[8] J. Antony. *Design of experiments for engineers and scientists*. Elsevier, 2nd edition, 2014.

[9] L. Eriksson, E. Johansson, N. Kettaneh-Wold, C. Wikström, and S. Wold. *Design of Experiments, Principles and Applications*. Umetrics AB, Sweden, 2000.

[10] H.B. Demuth, M.H. Beale, O. De Jess, and M.T. Hagan. *Neural Network Design*. Martin Hagan, USA, 2nd edition, 2014.

[11] T. Bäck. *Evolutionary algorithms in theory and practice*. Oxford University Press, 1996.

[12] Z. Michalewicz. *Genetic Algorithms + Data Structures = Evolution Programs*. Springer, 1996.

[13] V. Schramm, K. Willenborg, S. Kim, and S. Wittig. Influence of a honeycomb facing on the flow through a stepped labyrinth seal. In *ASME Turbo Expo 2000: Power for Land, Sea, and Air*, pages V003T01A092–V003T01A092. ASME, 2000. doi: 10.1115/2000-GT-0291.

[14] M.D. Morris. Factorial sampling plans for preliminary computational experiments. *Technometrics*, 33(2):161–174, 1991.

[15] B. Iooss and P. Lemaître. A review on global sensitivity analysis methods. In Dellino G. and Meloni C., editors, *Uncertainty Management in Simulation-Optimization of Complex Systems*, chapter 5, pages 101–122. Springer, 2015.

[16] F. Campolongo and J. Cariboni. Sensitivity analysis: How to detect important factors in large models. Technical report, 2007. http://publications.jrc.ec.europa.eu/repository/ handle/JRC37120.

[17] F. Pianosi, F. Sarrazin, and T. Wagener. A Matlab toolbox for global sensitivity analysis. *Environmental Modelling & Software*, 70:80–85, 2015. 10.1016/j.envsoft.2015.04.009.